

Drying Kinetics and Energy Consumption in Vacuum Drying Process with Microwave and Radiant Heating

M. Kamel^a, J.I. Lombrana^a, C. de Elvira^b and R. Rodríguez^a

^a Department of Chemical Engineering, Facultad de Ciencias, Universidad del País Vasco. Apdo. 644, 48080 Bilbao, Spain

^b Instituto del Frio (CSIC) Ciudad Universitaria. 28040 Madrid, Spain

Abstract The general objective of this work is to analyze energy input in a vacuum process with the incorporation of microwave heating. Thus, necessary criteria for designing an efficient freeze-drying operation are considered through the analysis of strategies based on the combination of different intensities of radiant and microwave heating. The other aim of this research topic is to study the kinetics of drying in relation to mass transfer parameters. Five freeze-drying strategies using both heating systems were used. Consequently, energy input could be related to diffusivity coefficients, temperature and pressure profiles during dehydration of the product and analyzed in comparison to a conventional freeze-drying process.

Keywords vacuum microwave drying, diffusivity constant, energy

1 INTRODUCTION

The main point in food drying is the reduction of the moisture content to a level that usually ranges from 1% to 5%, which avoid microbial spoilage and undesirable enzymatic reactions. High temperature and long drying time degrades the product's original color and causes a significant loss of characteristic flavor^[1], being common, as well, thermal degradation of nutritional substances.

As response to these problems, microwave technology has found increasing applications in process industries such as drying, tempering and pasteurization. Microwave (MW) heating produces a very rapid and low temperature drying, preventing the damage of the product. Several food properties, *e.g.* color and nutrient content, can be greatly preserved due to the absence of air. Owing to the use of vacuum, oxidation can be prevented as well. Microwave power and pressure can be manipulated to expand the structure of some products, yielding structure and texture that are unobtainable by other techniques^[2]. However, a major disadvantage is the high cost of the energy that is used in such applications. The MW heating offers, therefore, a good opportunity to increase the drying rate in comparison with conventional heating. However the MW freeze-drying application is limited due to plasma discharge problems. The appearance of this phenomenon produces a great energy loss resulting in an excessive heating on the dry zone of the material, damaging seriously the final product.

The liquid water has a dielectric factor much higher than the one for the ice, and every local melting on the frozen zone of the material generates a fast-

chained heating reaction that gives rise to the increase of temperature that can only be controlled by vacuum.

2 EXPERIMENTAL METHODS

Experiments were made using a high viscosity gel mixture of an aqueous Tylose (8%) and Sodium Sulfit (1.35%) solution. Gel product was arranged in spherical pieces of about 4.3 cm diameter. The inner temperature (frozen zone) was controlled in every experiment whereas the temperature in the dry zone was controlled only in certain cases. Two different types operational strategy were used:

Type I: The temperature of the superficial layer, T_s , was controlled to an assigned value of 40°C by grill heating. The corresponding frozen core temperature, T_c , was controlled by microwave heating.

Type II: Initially process is only heated by grill. Once superficial layer temperature reaches 0°C, microwave substitute grill and the sole heating device up to the end of drying only T_s temperature is controlled.

The temperature of the frozen zone of the product (T_c) and the operation strategy determined the specific conditions of each experiment. The drying of the spherical pieces was carried out in a glass container (inner diameter equals to 106 mm) that was introduced in the MW chamber and connected to the condenser and the vacuum pump using an experimental set-up described in a previous work^[3]. The vessel was hermetically closed with a glass cap of 0.8 mm depth. Three optic fiber probes were passed through the glass vessel cap in order to follow temperatures at: the outer layer (T_s), the frozen core (T_c), and the air inside the vessel (T_m). Five different experiments were

carried out. Table 1 shows the different conditions of each one and the different strategies used, concerning T_c and T_s control.

Table 1 Experiments carried out

Experiment	Type of strategy	Frozen temperature T_c , °C	T_s control
1	(I)	-8	Yes
2	(I)	-5	Yes
3	(II)	-10	No
4	(II)	-8	No
5	(II)	-5	No

An important part of this study is the estimation of the energy emitted by the MW generator and the radiant device, such as its evolution with time. As the MW power is too high for the mass to be dried and lack of power regulation, a charge that consists of 1 liter of water is used to absorb an important fraction of the energy. The system was stopped in order to check the evolution of the mass sample, the mass of evaporated water and its temperature. It was found that, in microwave systems when magnetron leads to an electric field higher than the threshold value, there was a "plasma" discharge phenomenon^[4]. It is possible to avoid this phenomenon by regulating the applied microwave power in the system, using on/off cyclic heating. Fig. 1 shows the on/off cyclic heating of microwave application combined with pressure modification. The high pressure is coincident with the time when microwave is active. In this case, on/off cycles of 8/18 for microwave application were used to control T_c .

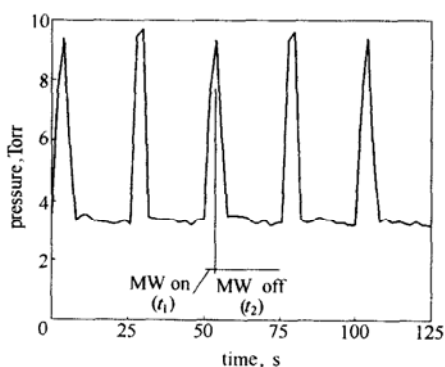


Figure 1 Microwave on/off cyclic heating (1Torr=133.3Pa)

To control T_s , on/off cycles 10/10 were used for grill heating application. Nevertheless, in this case no correspondence with cycles of pressure is necessary. Table 2 shows the number of times that each cycle was activated and the relation with chosen strategy. Figs. 2 and 3 show MW and Grill evolution vs time for the experiments of the strategies I and II respectively.

Table 2 Relation with G10/10 and MW 8/18 (Experiment 1 of type I strategy)

Time min	G10/10	MW8/18	Time min	G10/10	MW8/18
0	0	0	240	700.5	130.64
30	118	0.397	270	746	148.38
60	360	9.913	300	760	176.12
90	491	18.26	330	772.5	228.28
120	575	33.42	360		300.27
150	604.5	54.05	390		362.74
180	639.5	77.876	420		434.74
210	682.5	105.7	450		479.22

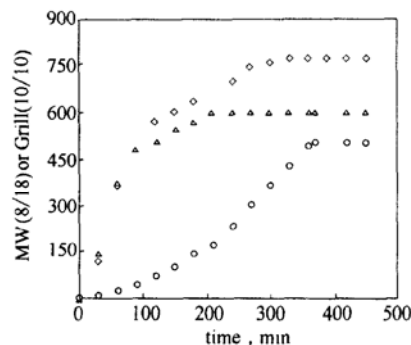


Figure 2 Number of heating cycles for MW and grill application in type I experiments

◇ Exp.1(Grill); □ Exp.1(MW);
△ Exp.2(Grill); ○ Exp.2(MW);

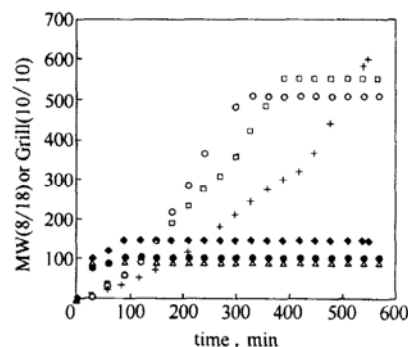


Figure 3 Number of heating cycles for MW and grill application in type II experiments

◆ Exp.3(Grill); + Exp.3(MW); △ Exp.4(Grill);
□ Exp.4(MW); ● Exp.5(Grill); ○ Exp.5(MW);

An important target of this work deals with the energy of freezing analysis of power application during different drying strategies. Only a part of the total supplied electrical energy (microwave plus grill) is absorbed during drying process (E_{drying}) and can be expressed according to Eq. (1):

$$E_{drying} = E_{total} - (E_{charge} + E_{losses}) \quad (1)$$

E_{charge} is the energy used for heating and water vaporization of the charge, while E_{losses} means the energy loss either by heat convection or electrical to heat conversion. The E_{charge} was estimated following the mass

and temperature of the water charge. Parallel experiments were conducted to estimate the convective coefficient using MW heating only, and MW with Grill together. Values of 18 and 35 W·m⁻²·°C were obtained respectively for both situations in order to determine the heat dissipated by convection.

An effective energy ratio is defined as: $E_{\text{drying}}/(E_{\text{drying}} + E_{\text{charge}})$. The results are plotted in the Fig. 4 for every experiment. The effective energy is much poorer when the Grill is used than when the MW was applied alone. The energy absorbed by the product that was used to increase its temperature level and water evaporation was calculated as:

$$E_{\text{drying}} = m_T C_P \Delta T + \lambda_V m_{\text{vap}} \quad (2)$$

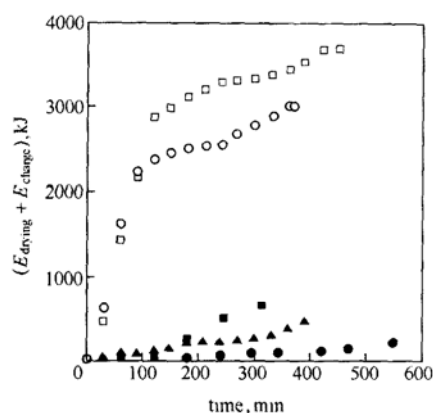


Figure 4 Effective energy versus time
● Exp.3; ▲ Exp.4; ■ Exp.5; □ Exp.1; ○ Exp.2;

Table 3 shows the relation between MW the absorbed energy for drying and the total absorbed heat energy ($E_{\text{drying}} + E_{\text{charge}}$). Experiments follow the order of increase in values of $E_{\text{drying}}/(E_{\text{drying}} + E_{\text{charge}})$.

Table 3 Losses and energy relations

Experiment	Type of strategy	Absorbed energy, kJ	$E_{\text{abs}}, \text{kJ}$	$E_{\text{drying}}/E_{\text{ABS}}$
3	(II)	94.343	179.359	0.526
4	(II)	84.830	398.262	0.213
5	(II)	85.086	531.787	0.160
1	(I)	85.299	1015.464	0.084
2	(I)	88.454	1092.024	0.081

The efficiency of the process is much higher when the MW is used alone, so the use of Grill is not recommendable in a general sense. The uses of MW power as the heating mean greatly reduces the energy consumption and heat losses. When type I strategies are used the energy efficiency is very similar for all the experiments, which shows the control temperature of the frozen zone hardly affects it. On the other hand, when type II strategy is used the efficiency is higher at lower temperature, going from 0.526 to 0.160.

3 DIFFUSIVITY ANALYSIS

In a MW vacuum drying, the moisture release is not only by sublimation, but there is a continuous gradient of moisture through the material. With the aim of a comparative analysis, a model with this particular assumption of mass transfer is used to describe the kinetics of the process^[5].

The molecular diffusion is usually admitted to be the main moisture transfer mechanism in drying^[6]. The drying kinetics are, therefore, usually represented by Fick's law of diffusion, the solution of which depends on the initial and boundary conditions considered, on whether the diffusion coefficient is considered to be constant or varying, and on the shape of the particle (Shivhare, 1994). For particles with spherical geometry:

$$\frac{\partial M}{\partial t} = D_M \frac{1}{r^2} \frac{\partial}{\partial r} \left(r^2 \frac{\partial M}{\partial r} \right) \quad (3)$$

The analytical solution for a homogeneous sphere with a constant diffusion coefficient, assuming no volume variation, was obtained by Crank^[7]:

$$MR = \frac{6}{\pi^2} \sum_{n=1}^{n=\infty} \frac{1}{n^2} \exp \left[-\frac{n^2 \pi^2 D_M t}{R_c^2} \right] \quad (4)$$

where

$$MR = \frac{M - M_{\text{eq}}}{M_o - M_{\text{eq}}} \quad (5)$$

The initial and limit conditions considered are:

$$M = M_o \quad \text{when} \quad r \leq R, t = 0 \quad (6)$$

$$M = M_{\text{eq}} \quad \text{when} \quad r = R, t \geq 0 \quad (7)$$

$$\frac{\partial M}{\partial r} = 0 \quad \text{when} \quad r = 0, t > 0 \quad (8)$$

The theoretical MR values were calculated by equation 4 until the best fitting with the experimental ones is reached. Figs. 5 and 6 show that the drying rate is higher for type II than for type I. Comparing samples within the same model, it is observed a faster rate drying for higher temperature of the frozen zone. The experiments 1 and 4 are plotted together to show their fitting to the kinetic model (Fig. 6).

In Fig. 6, in order to obtain an adequate fitting of experimental evolution in the last drying period, the beginning of theoretical curve is retarded 90 minutes due to well defined water removing mechanisms during early drying. The water removed is mainly unbound water until the values of experimental and theoretical MR are coincident, and this will be the most important mechanism during the first period. The critical moisture (MRC) in which experimental and theoretical

moisture are coincident defines the moment in which the diffusional resistance become significant. Table 4 shows the delay times for the different samples, the critical MR value (MRc) and the diffusivity values, corresponding to the last diffusional period.

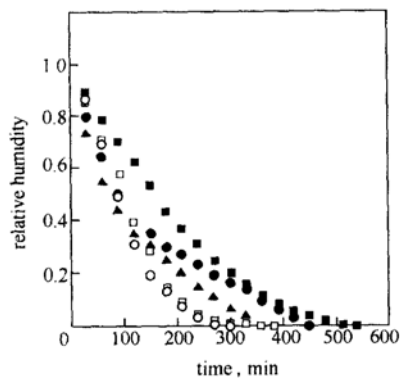


Figure 5 MR versus time for the type I and II strategy

● Exp.1; ▲ Exp.2; ■ Exp.3; □ Exp.4; ○ Exp.5;

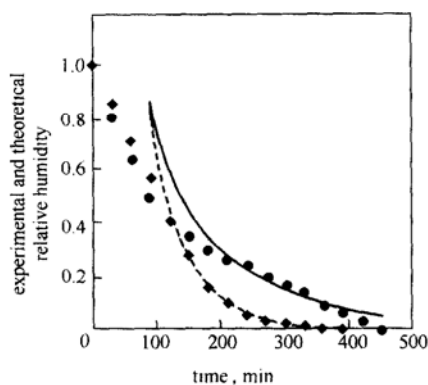


Figure 6 Experimental and theoretical relative humidity versus time

● Exp.1 (Exp); — Exp.1 (Theo);
◆ Exp.4 (Exp); - - - Exp.4 (Theo);

Table 4 Delay time, MRc and diffusivity for each experiment

Experiment	Delay time, h	MRc	Diffusivity, $\text{cm}^{-2}\cdot\text{h}^{-1}$
1	1.5	0.27	0.34
2	1.0	0.30	0.42
3	3.0	0.23	0.49
4	1.5	0.40	0.75
5	1.5	0.20	0.95

Table 4 shows that diffusivity values are higher for strategy type II. The higher the temperature of the frozen zone the higher the diffusivity. The trend for the MRc value is not well understood, but it seems to be a maximum at -8°C . The delay time is slightly dependent on the frozen zone temperature, being the delay time higher the lower the temperature.

4 PRESSURE AND TEMPERATURE EVOLUTION

The pressure and temperature evolution along time was studied. The samples at -8°C are plotted to extract possible similarities and differences.

Figures 7 and 8 show that there is an increase in the pressure level during the initial period. Then, the pressure level remains fairly constant, below the triple point of water. The initial period ends when there is no unbound water and then a diffusional second period begins.

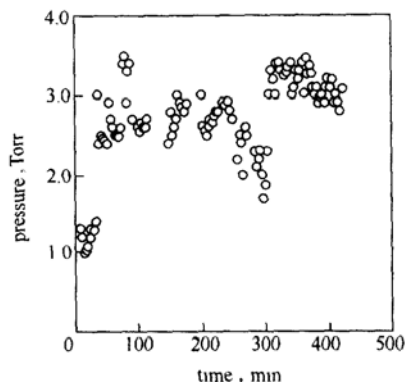


Figure 7 Pressure evolution for the sample 1

○ Exp.1 (1Torr=133.3 Pa)

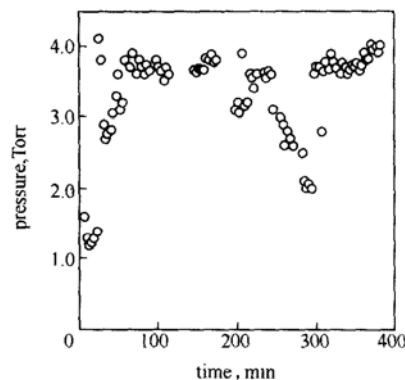


Figure 8 Pressure evolution for the sample 4

○ Exp.4 (1Torr=133.3 Pa)

Characteristic temperature and pressure levels can be related to the first and the second period. Thus, during the first period temperature is below 0°C and begin to rise when the second period starts (Figs. 9 and 10).

5 COMPARISON BETWEEN MW AND CONVENTIONAL HEATING

A conventional freeze-drying experiment is made to compare it with the MW experiments. The temperature of the dry zone was controlled at 40°C and the temperature of the frozen zone at -8°C . The comparison is made with the experiment at the same frozen zone temperature and using the more advantageous strategy II. Fig. 11 shows the evolution of the

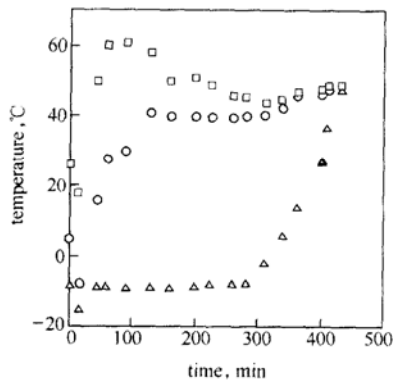


Figure 9 Temperature evolution for the sample 1
 ΔT_c ; $\square T_m$; $\circ T_s$

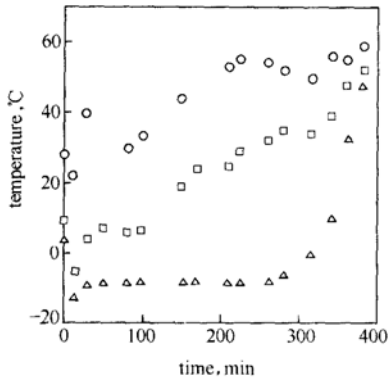


Figure 10 Temperature evolution for the sample 4
 ΔT_c ; $\square T_s$; $\circ T_m$

humidity versus time for both experiments. Fig. 11 shows that there is a reduction of time higher than 50% when MW heating is used instead of conventional heating. However, in this case one should compare only time values until a humidity equals to 5% is reached, because from this humidity to the end, the process was speeded up by increasing the heating power in order to reduce the final drying time. Therefore the time reduction is equal to 65%, in other words, 1100 min in conventional heating and only 280 min in MW heating.

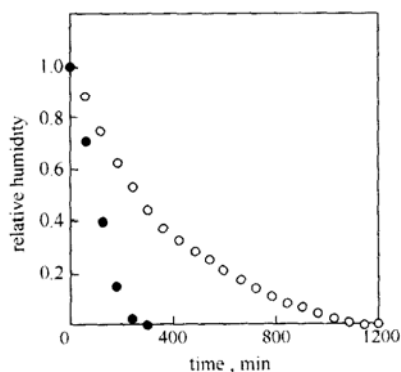


Figure 11 Relative humidity evolution versus time for conventional and MW drying
 \circ conventional freeze drying; \bullet MW

6 CONCLUSIONS

An increase in the frozen zone temperature improves the drying kinetics as is shown in the increase of the diffusivity coefficients. Consequently, using MW heating reduces more than 65% of the drying time with respect to the conventional heating. It was proved that when MW heating is used alone the energy efficiency is higher than when the MW heating is combined with the radiant heating. The energy efficiency using MW heating is improved working with temperatures in the range of melting but if a considerable frozen state (lower temperatures) is kept.

NOMENCLATURE

C_p	constant pressure conductivity, $J \cdot g^{-1} \cdot ^\circ C$
D_M	water diffusivity through the solid, $cm^2 \cdot s^{-1}$
M	humidity (dry basis), $g \cdot g^{-1}$ (water to solid)
MR	relative humidity
M_{eq}	equilibrium humidity (dry basis), $g \cdot g^{-1}$ (water to solid)
M_{evap}	evaporated mass, g
M_T	total mass, g
M_o	initial humidity (dry basis), $g \cdot g^{-1}$ (water to solid)
R_e	equivalent radius, m
r	radius, m
T	temperature, $^\circ C$
t	time, s
λ_v	vaporization heat, $J \cdot g^{-1}$

Subscripts

e	equivalent
eq	equilibrium
o	initial

REFERENCES

- Yongsawatdigul, J., Gunasekaran, S., "Microwave-vacuum drying of cranberries (I) Energy and efficiency", *Journal of food processing and preservation*, **20**, 121–143 (1996).
- Lin, T.M., Durance, T.D., Scaman, C.H., "Characterization of vacuum microwave, air and freeze dried carrot slices", *Food Research International*, **31**, 111–117 (1998).
- Lombrana, J.I., Zuazo, I., Izkara, J., "Moisture diffusivity behavior in freeze drying under microwave heating power application", *Drying Technol.*, **19** (8), 1613–1627 (2001).
- Izkara, J., Lombrana, J.I., "Cycled pressure control for an efficient microwave heating in freeze-drying", In: *Drying'96*, Elsevier Science Publishers Ltd, 1385–1392 (1996).
- Shivare, U.S., Raghavan, G.S.V., Bosisio, R.G., "Modeling the drying kinetics of maize in a microwave environment", *Journal Agricultural Engineering Research*, **57**, 199–205 (1994).
- Brooker, D.B., Bakker-Arkema, F.W., Hall, C.W., *Drying Cereal Grains*, Avi Publication (1974).
- Crank, J., *The Mathematics of Diffusion*, Oxford University Press (1975).